

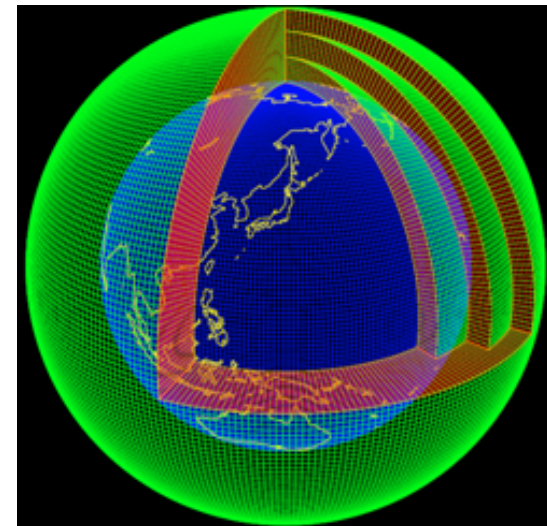
Uncertainties in future changes in tropical cyclone activity projected by multi-physics and multi-SST ensemble experiments

Hiroyuki Murakami (University of Hawaii/MRI)

Murakami *et al.* (2012, *Clim. Dyn.*)

Outline

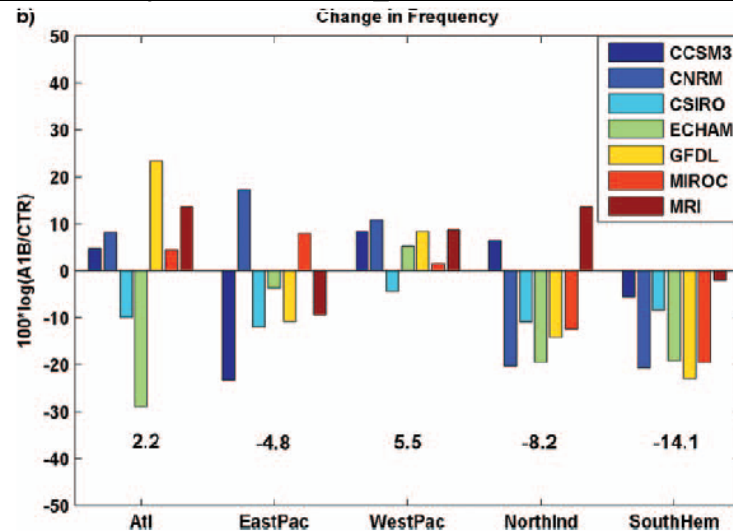
- Motivation
- Methodology for multi-physics and multi-SST ensemble experiments
- Results
- Summary



20 km-mesh grids

Motivation

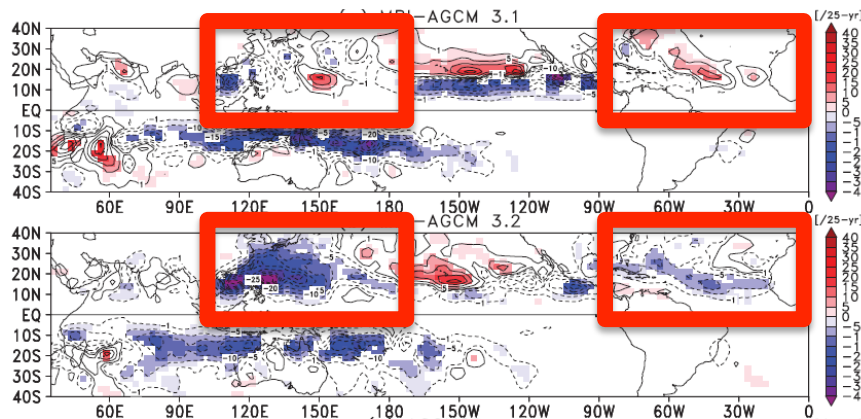
Uncertainty due to prescribed SSTs



Emanuel et al. (2008, *BAMS*)

Different future SST causes different sign of projected changes in TC genesis number in a specific basin.

Uncertainty due to model physics



Murakami et al. (2012, *J. Climate*)

Different cumulus convection scheme causes different sign of projected changes in TC frequency of occurrence in a specific basin.

Which of SST or cumulus convection scheme causes uncertainty largely?
A key factor is to derive robust signals across different exp. settings.

Multi-model & Multi-SST Ensemble Projections using 60-km-mesh model

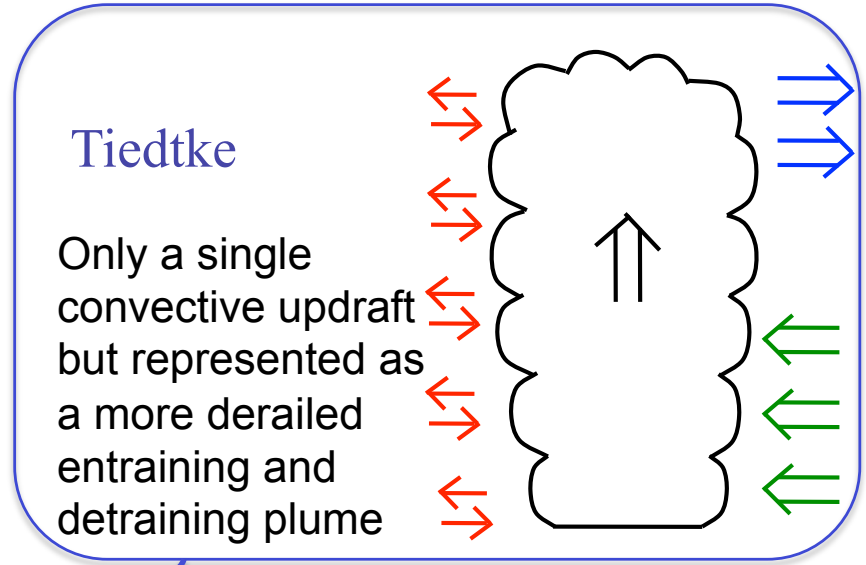
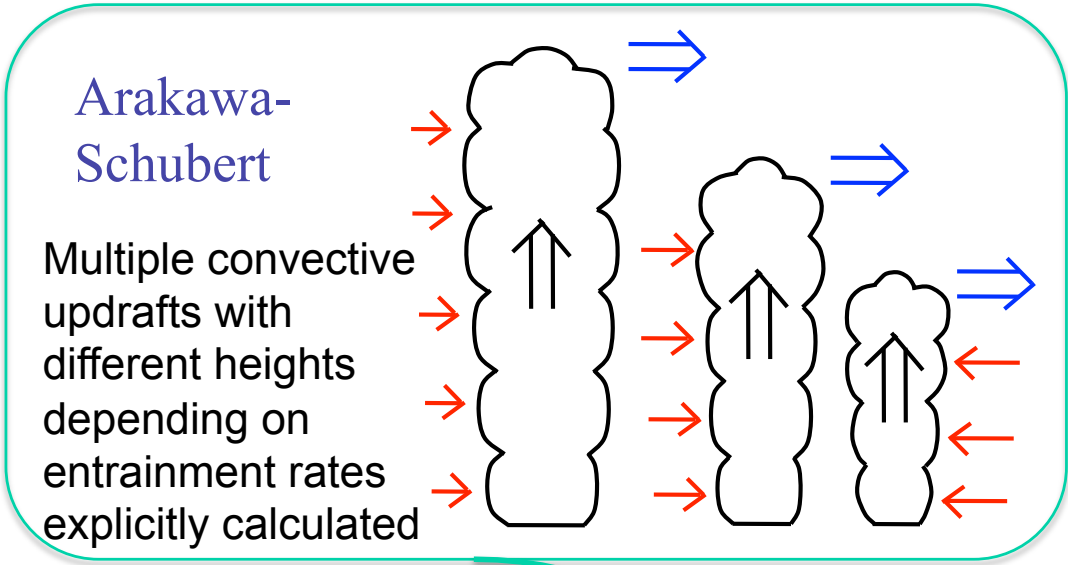
▪ Using 60-km-mesh MRI-AGCM, 12 ensemble future (2075-2099) experiments were conducted.

3 (cumulus) × 4 (SST) = 12 ensemble experiments

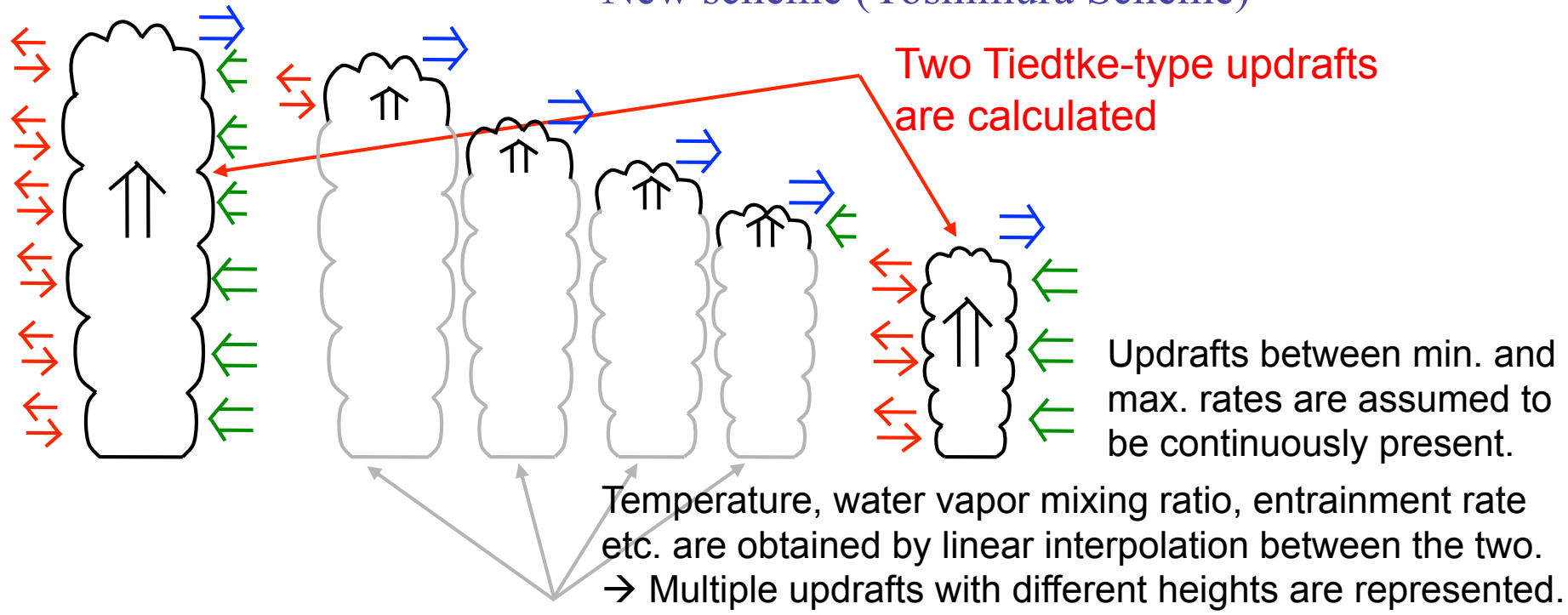
Abbreviation	Cumulus Convection Scheme	Prescribed Future SST
Y0	Yoshimura Scheme (YS)	18 CMIP3 Models Ensemble Mean
Y1	Yoshimura Scheme (YS)	Cluster 1
Y2	Yoshimura Scheme (YS)	Cluster 2
Y3	Yoshimura Scheme (YS)	Cluster 3
K0	Kain-Fritsch Scheme (KF)	18 CMIP3 Models Ensemble Mean
K1	Kain-Fritsch Scheme (KF)	Cluster 1
K2	Kain-Fritsch Scheme (KF)	Cluster 2
K3	Kain-Fritsch Scheme (KF)	Cluster 3
A0	Arakawa-Shubert Scheme (AS)	18 CMIP3 Models Ensemble Mean
A1	Arakawa-Shubert Scheme (AS)	Cluster 1
A2	Arakawa-Shubert Scheme (AS)	Cluster 2
A3	Arakawa-Shubert Scheme (AS)	Cluster 3
YG	Yoshimura Scheme (YS)	1.83K uniform warming

Three types of physics used for multi-physics exp.

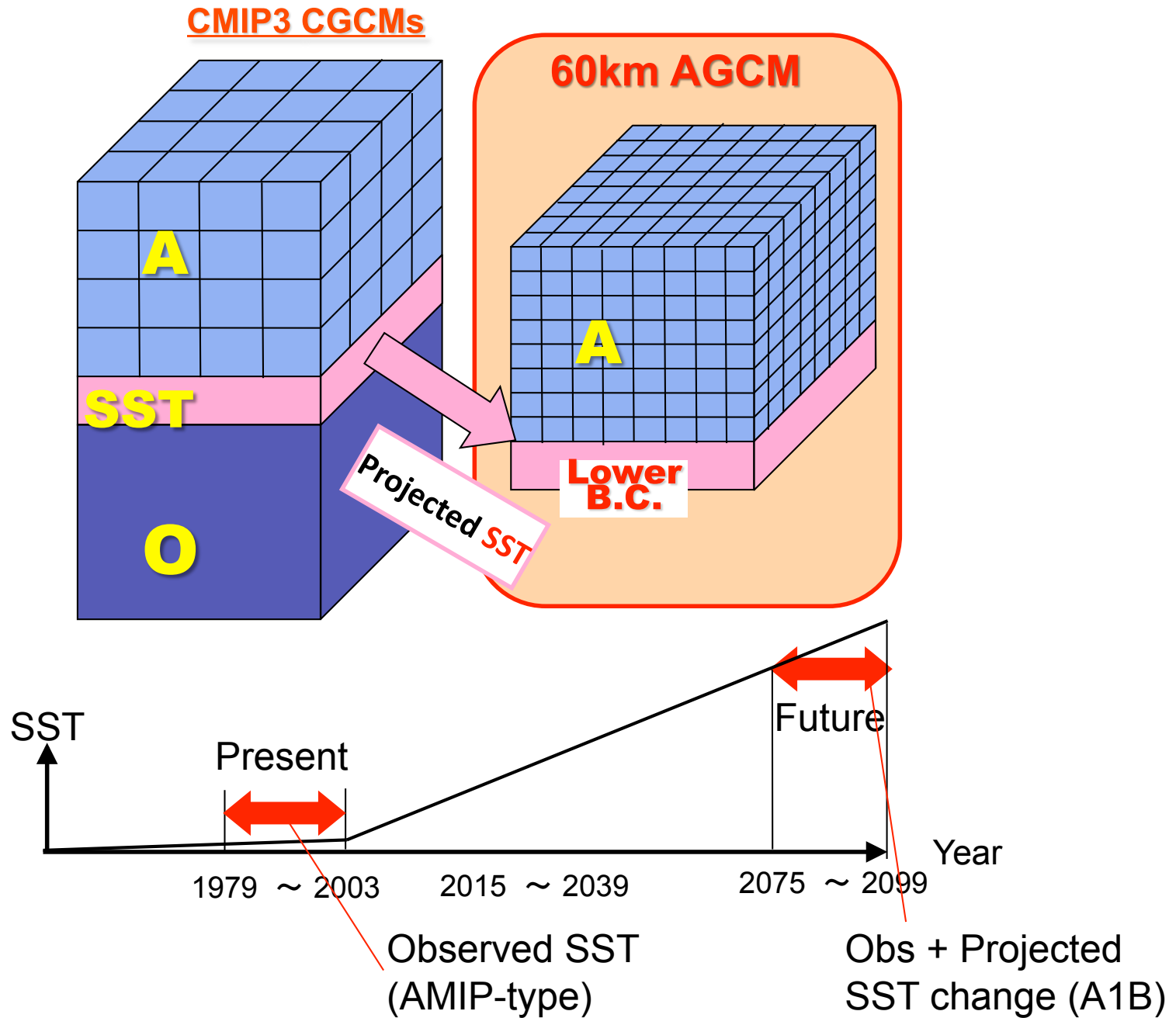
	MRI-AGCM 3.2 AS	MRI-AGCM 3.2 KF	MRI-AGCM 3.2 YS
Horizontal resolution	T _L 319 (60km)		
Vertical resolution	64 levels (top at 0.01hPa)		
Time integration	Semi-Lagrangian		
Time step	20 minutes		
Cumulus convection	Prognostic Arakara-Schubert	Kain-Fritsch	Yoshimura (Tiedtke-based)
Cloud	Tiedtke (1993)		
Radiation	JMA (2007)		
GWD	Iwasaki et al. (1989)		
Land surface	SiB ver0109 (Hirai et al.2007)		
Boundary layer	MellorYamada Level2		
Aerosol (direct)	5 species		
Aerosol (indirect)	No		



New scheme (Yoshimura Scheme)

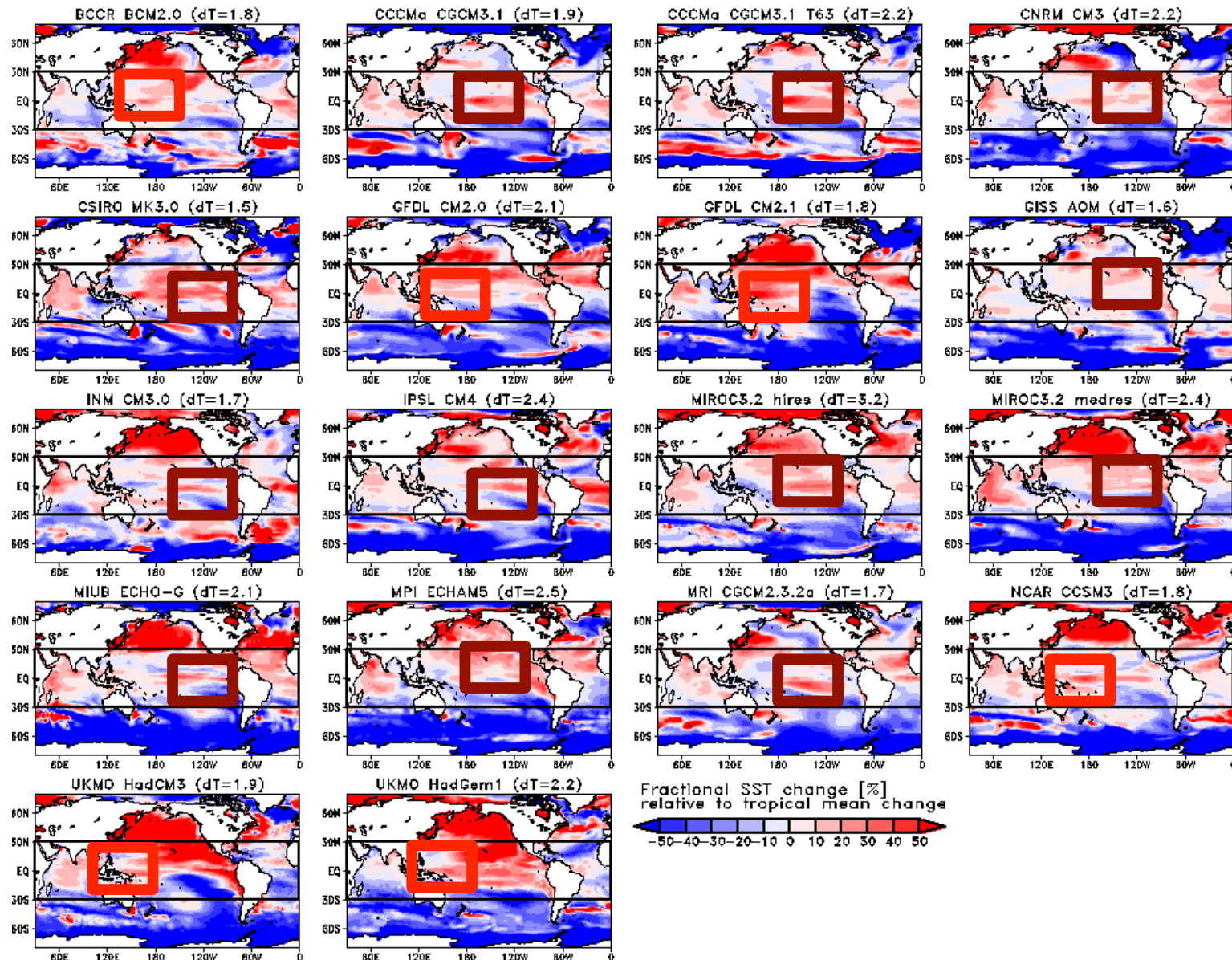


Time Slice Experiments

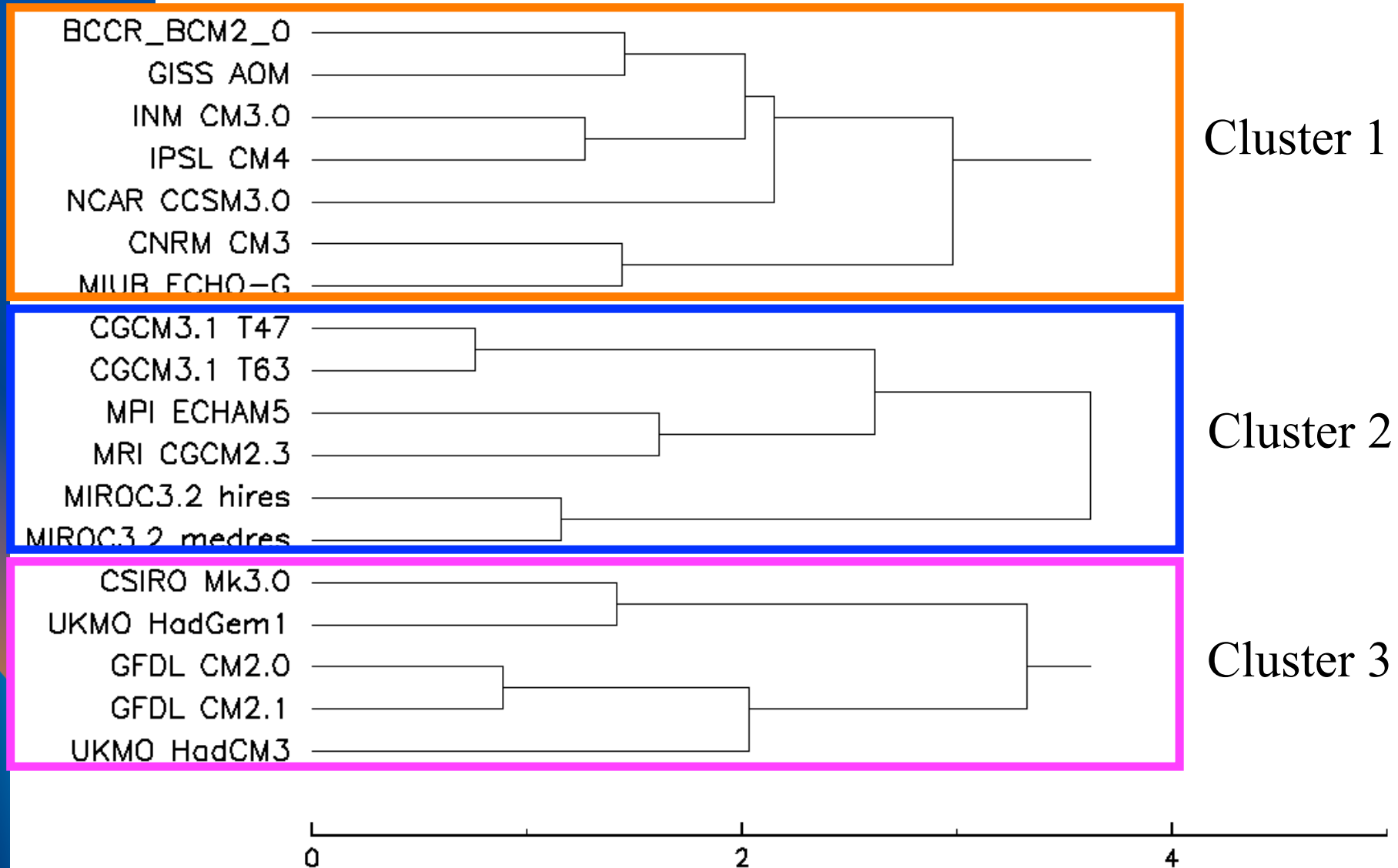


Multi-SST Ensemble Projections

Fractional SST change relative to tropical mean change in CMIP3 models under A1B scenario.



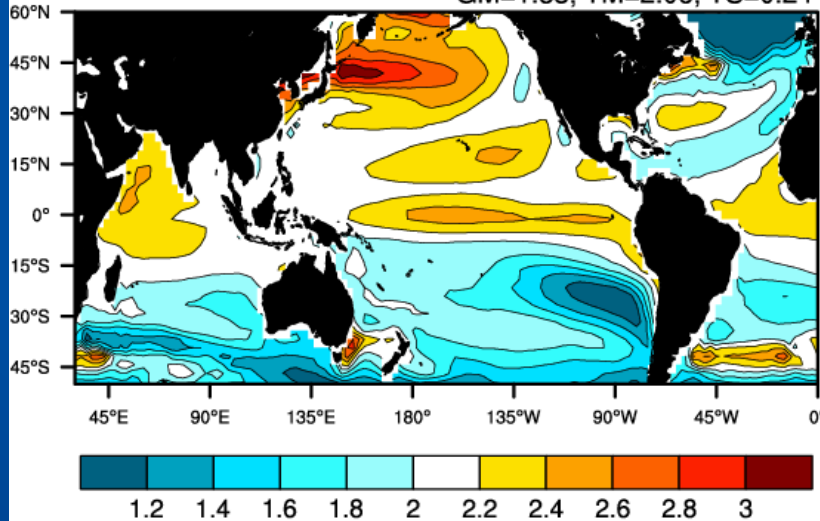
Multi-SST Ensemble Projections



Multi-SST Ensemble

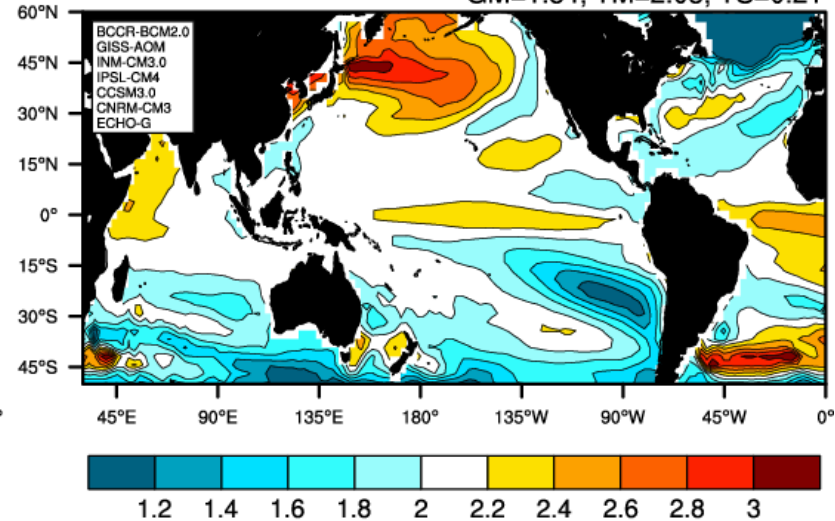
(a) CMIP3 Mean SST

GM=1.83, TM=2.06, TS=0.24



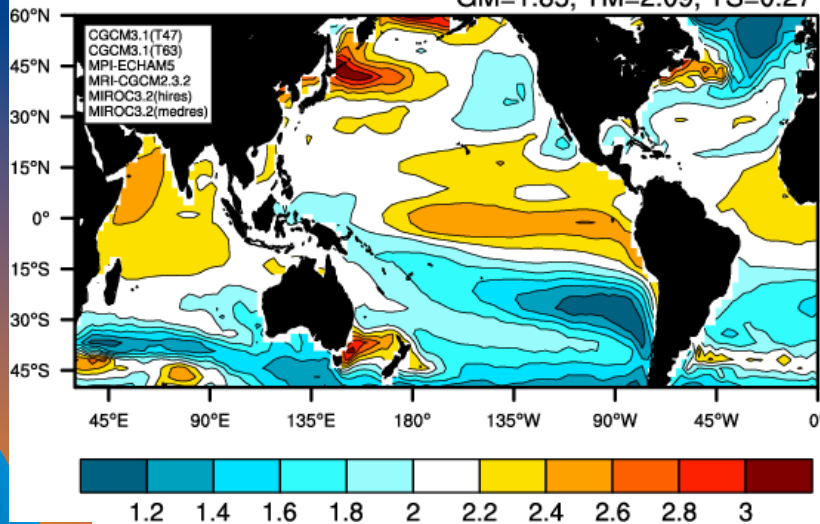
(b) Cluster1 SST

GM=1.84, TM=2.05, TS=0.21



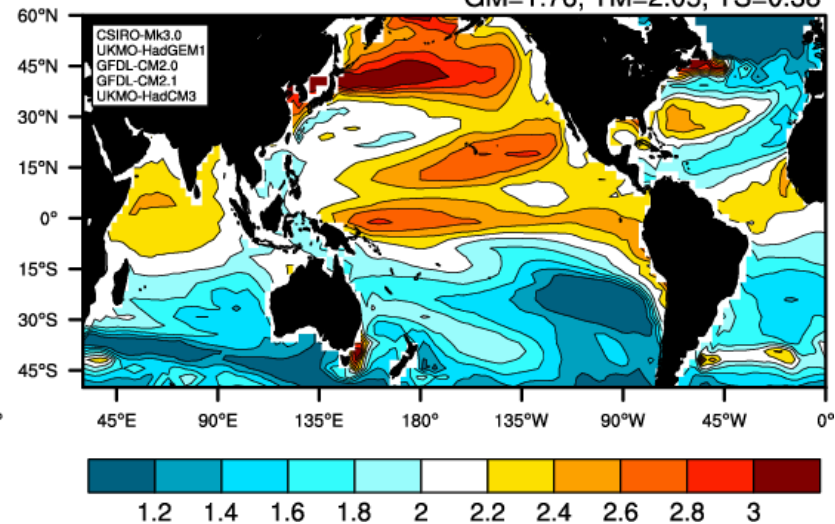
(c) Cluster2 SST

GM=1.85, TM=2.09, TS=0.27



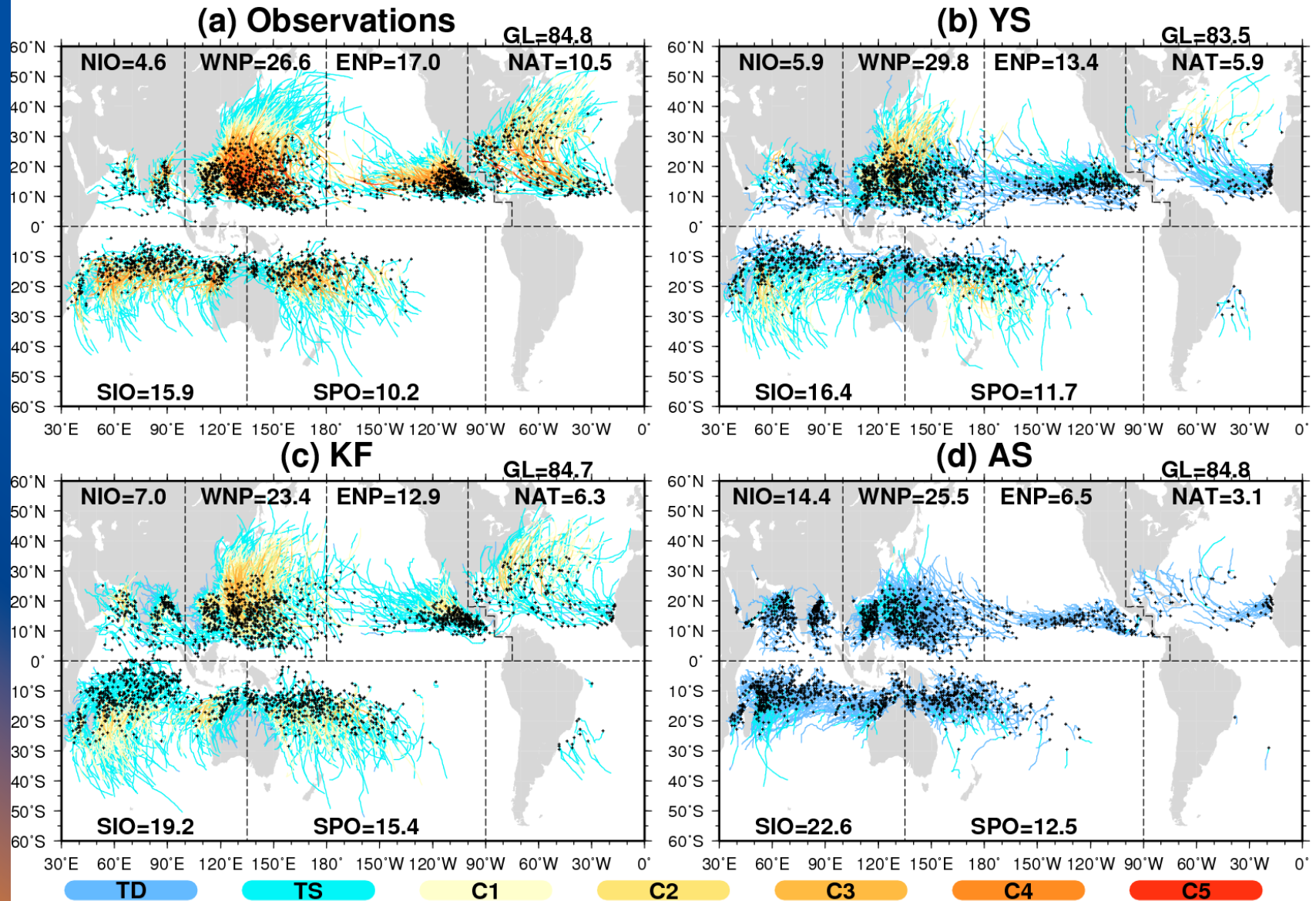
(d) Cluster3 SST

GM=1.76, TM=2.05, TS=0.38



Cluster 1 shows small spatial variance in tropics, while Cluster 3 SST shows large spatial variance in tropics.

Performance of control simulations

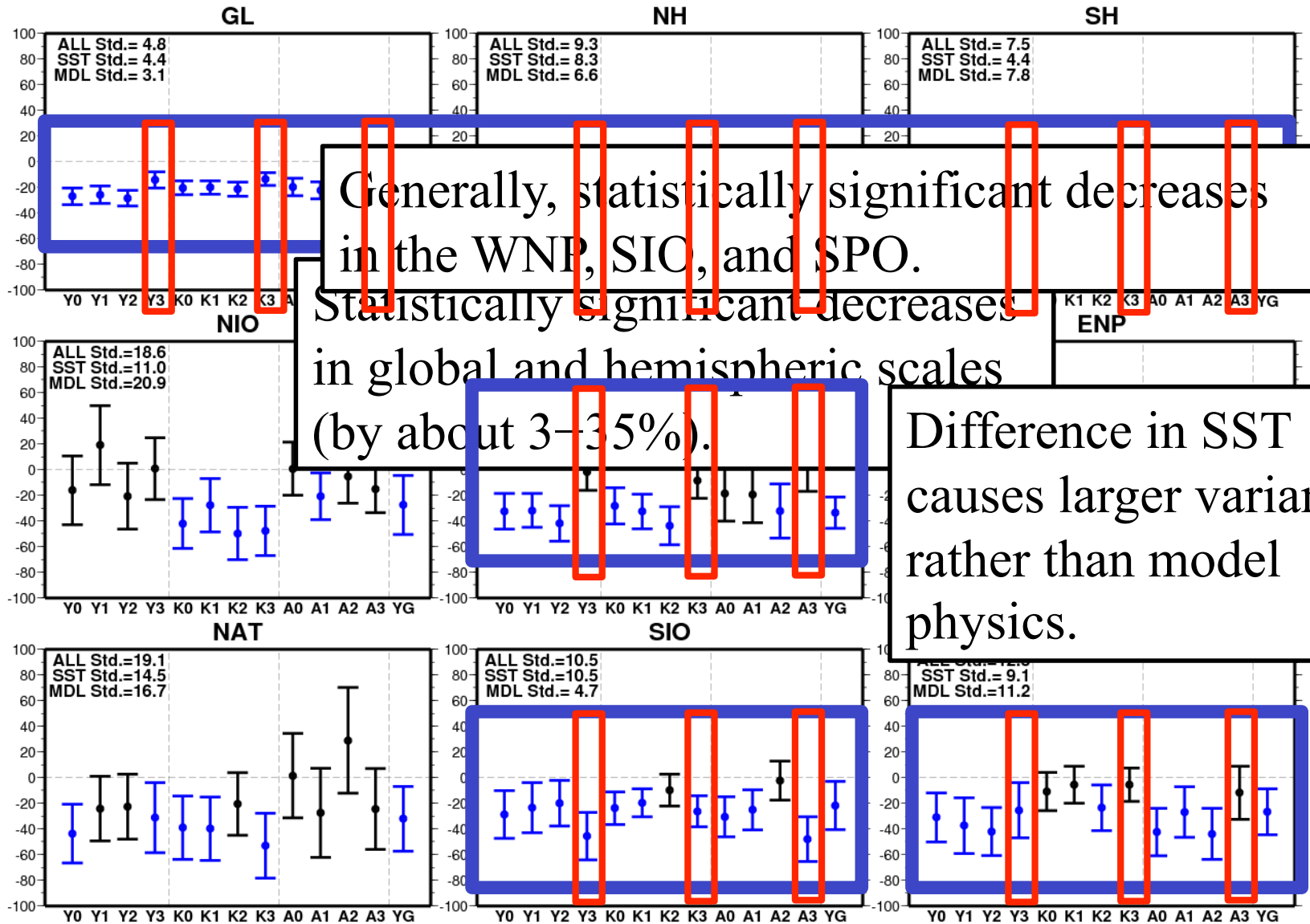


The YS and KF simulate reasonable TC global distribution, whereas AS has pronounced biases.

Future changes in TC number [%]

Y: Yoshimura, K:Kain-Fritsch, A: Arakawa Shubert

0: CMIP3 mean SST, 1:Cluster 1, 2:Cluster 2, 3: Cluster 3, G: Global uniform



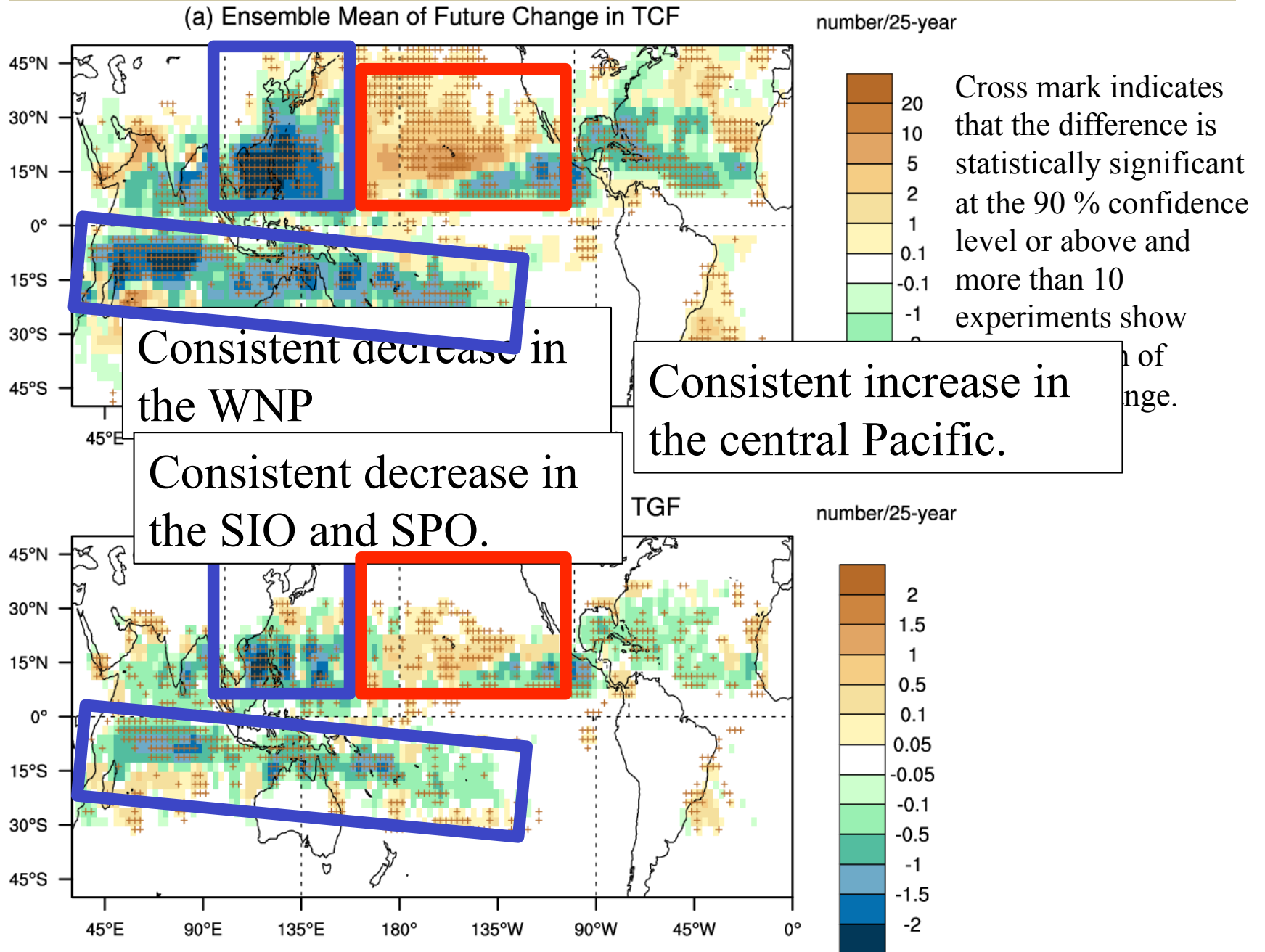
Generally, statistically significant decreases in the WNP, SIO, and SPO.

Statistically significant decreases in global and hemispheric scales (by about 3-35%).

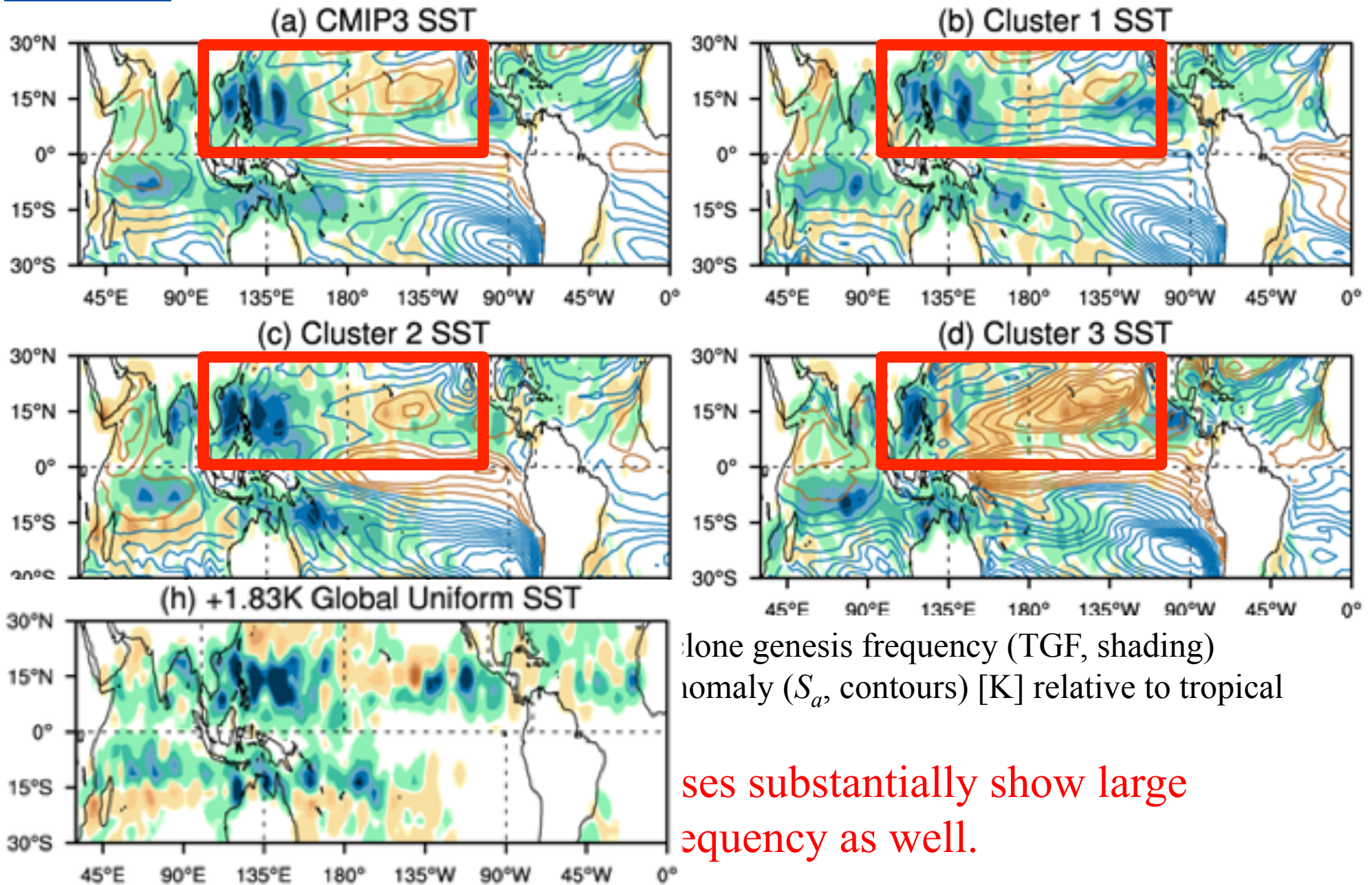
Difference in SST causes larger variances rather than model physics.

Future changes in TC frequency of occurrence and TC genesis frequency

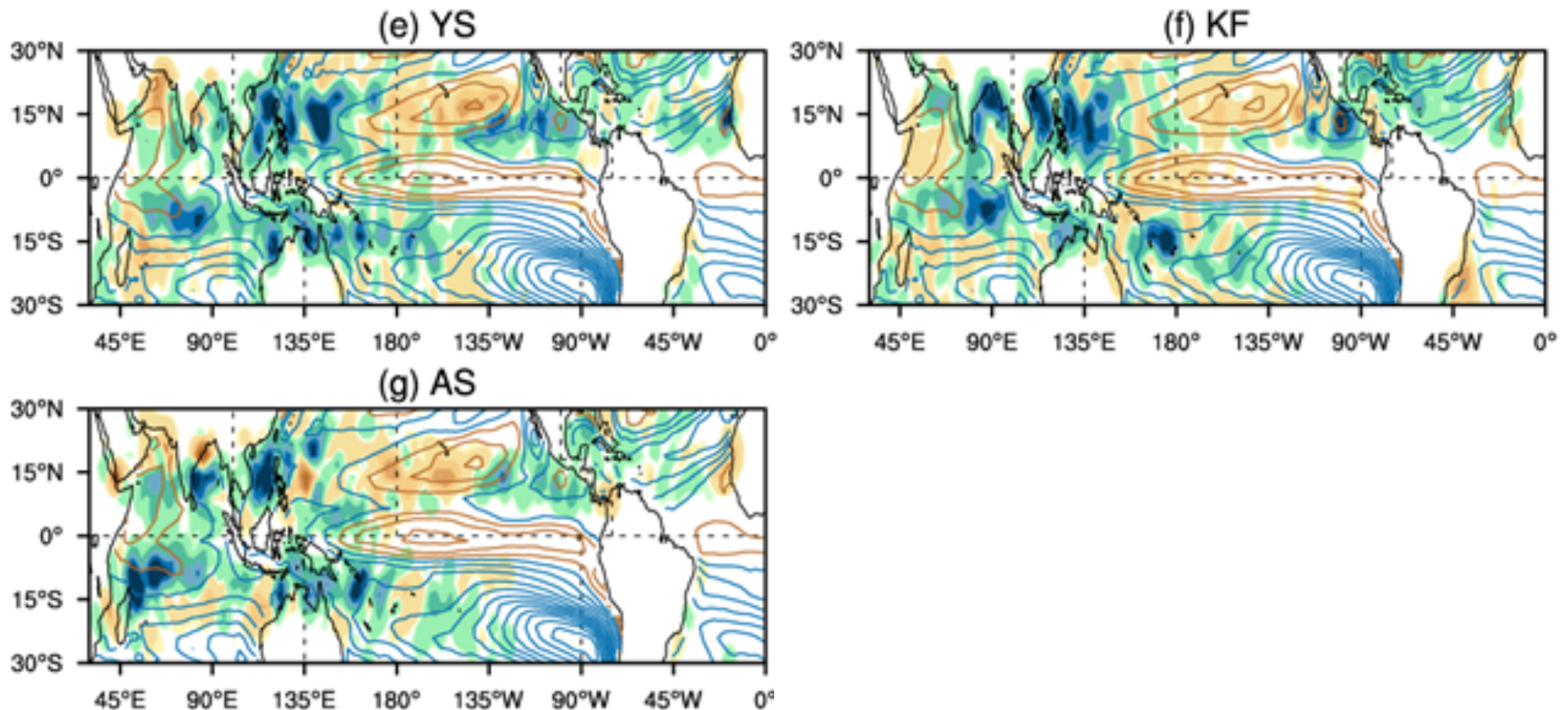
(a) Ensemble Mean of Future Change in TCF



Future changes in TC genesis frequency and SST



Future changes in TC genesis frequency and SST



Ensemble mean of future changes in tropical cyclone genesis frequency (TGF, shading) [number/25-year] and sea surface temperature anomaly (S_a , contours) [K] relative to tropical (30°S-30°N) mean.

Projected future changes in TC genesis frequency are relatively independent of the chosen cumulus convection scheme.

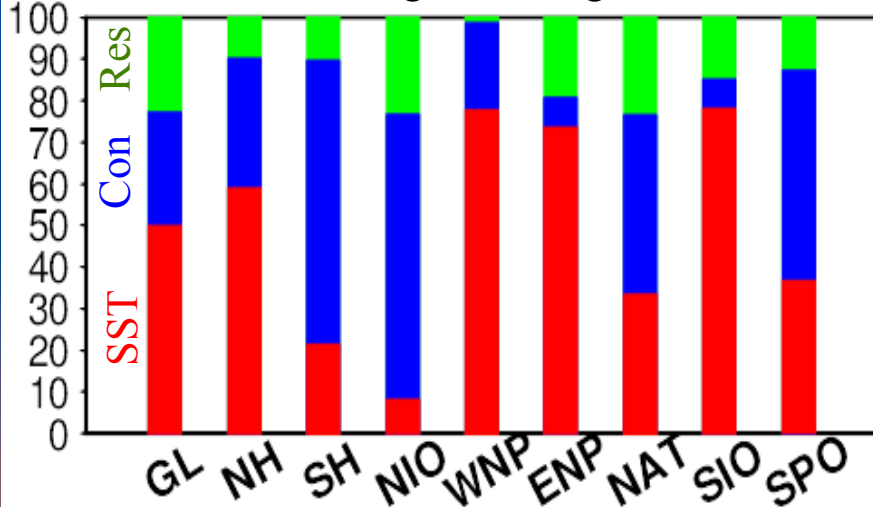
Responsible factor for inter-experimental variance

A two-way analysis of variance (ANOVA)

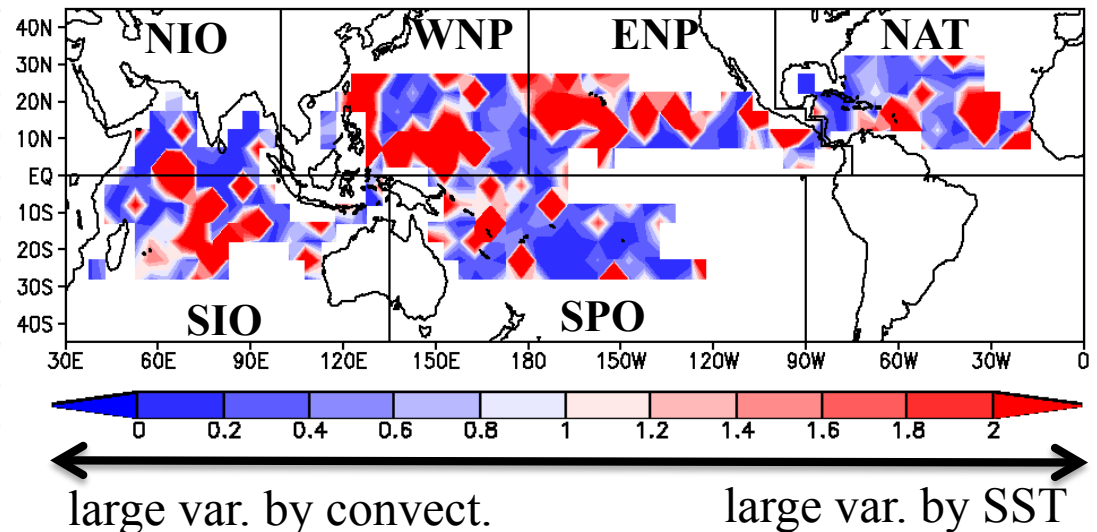
$$\sum_{i=1}^a \sum_{j=1}^b (X_{ij} - \bar{X}_{..})^2 = b \sum_{i=1}^a (\bar{X}_{i.} - \bar{X}_{..})^2 + a \sum_{j=1}^b (\bar{X}_{.j} - \bar{X}_{..})^2 + \sum_{i=1}^a \sum_{j=1}^b (X_{ij} - \bar{X}_{i.} - \bar{X}_{.j} + \bar{X}_{..})^2$$

All variance = **Variance by diff. in SST** + **Variance by diff. in convection schemes** + **Residual**

[%] Variance in changes in TC genesis number



TC genesis frequency : var (SST) / var(convect.)



- Difference in SSTs causes substantial inter-experimental variance in projected changes in TC genesis number.
- North Indian Ocean, North Atlantic, and South Pacific show substantial variance caused by difference in the cumulus convection schemes.

Conclusion

In order to evaluate uncertainties, we conducted multi-SST and multi-model ensemble projections.

- (a) Every ensemble simulation **commonly** shows **decrease in global and hemispheric TC genesis numbers by about 5-35%** under the global warming environment regardless of the difference in model cumulus convection schemes and prescribed SSTs.
- (b) All experiments tend to project future **decreases** in the number of TCs **in the western North Pacific (WNP), South Indian Ocean (SIO), and South Pacific Ocean (SPO)**, whereas they commonly project **increase** in the **central Pacific**.
- (c) Future changes in spatial distribution of **SST** are **major source of uncertainty** in terms of future changes in TC genesis. Further SST ensemble experiments may be necessary for minimizing uncertainty.

Thank you!



At Yankee Stadium (Sunday)

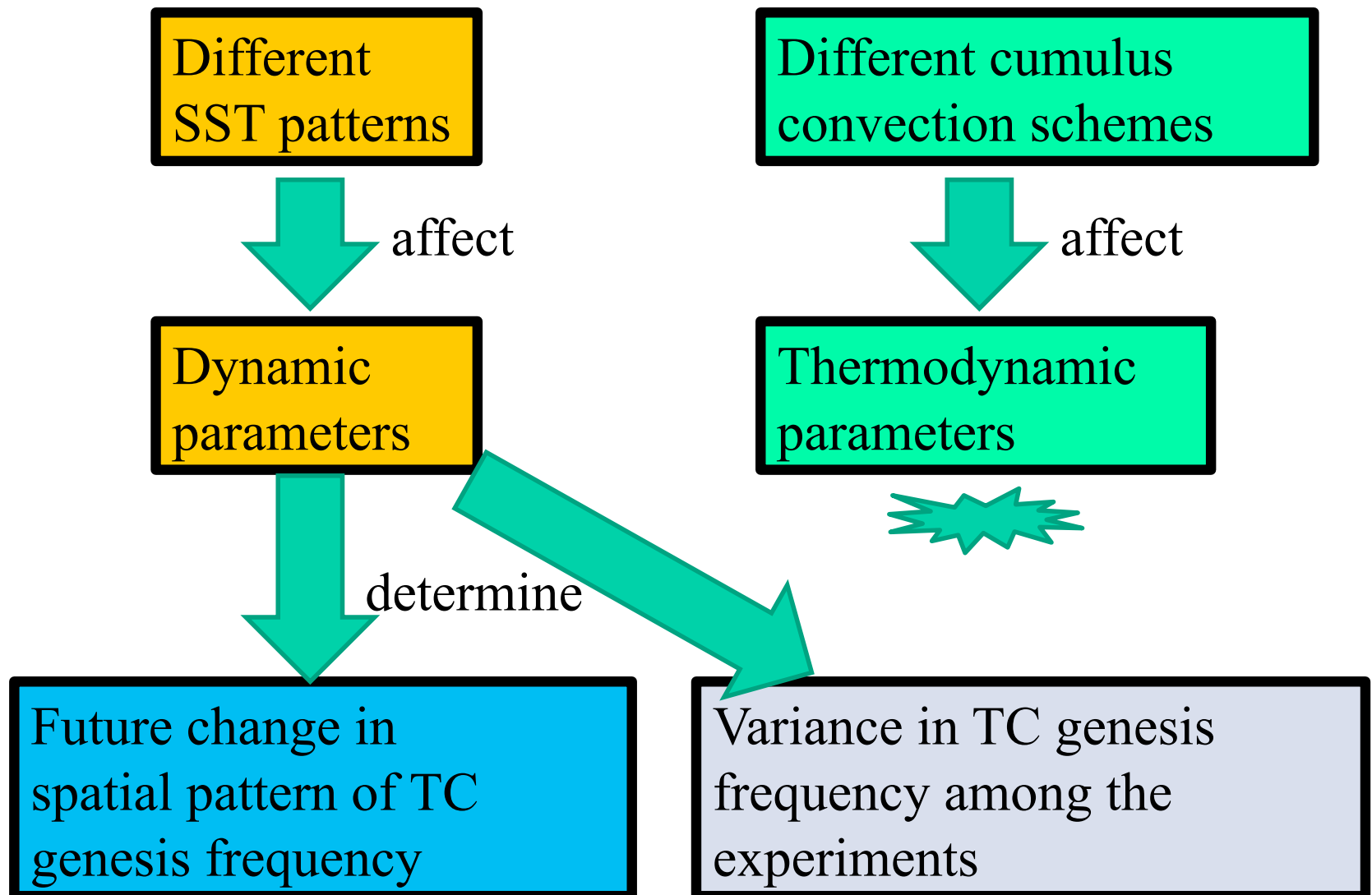


At Statue of Liberty
(Yesterday)



and Princeton

Summary of statistical analysis

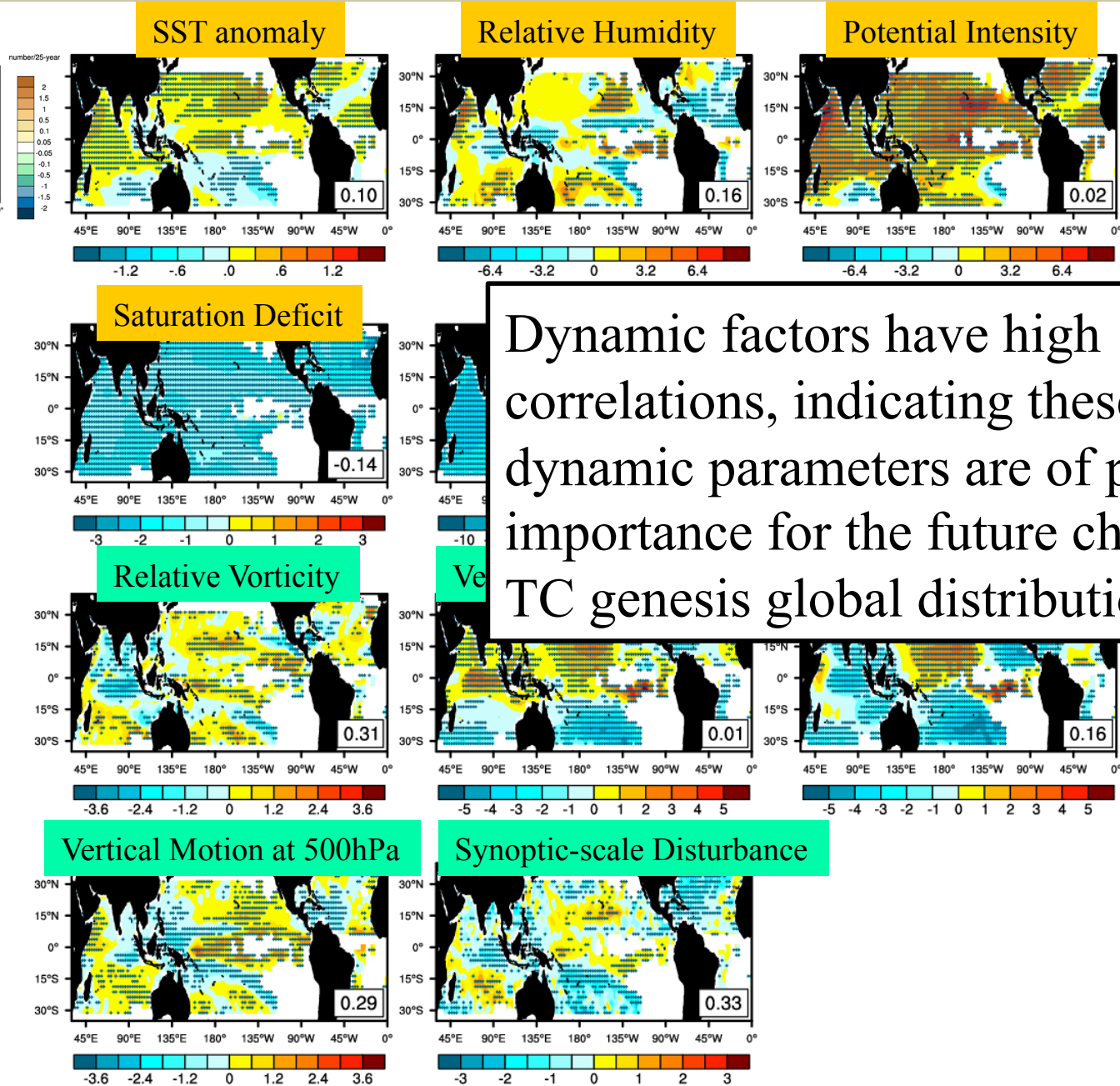
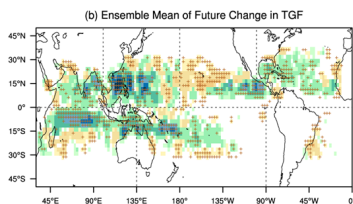


Spatial variation in SST is a source of uncertainty in projecting future changes in TC genesis frequency through responses of dynamical factors. Further SST ensemble experiments are necessary to minimize those uncertainties.

Reference

- Murakami, H., and co-authors, 2011: Future changes in tropical cyclone activity projected by the new high-resolution MRI-AGCM. *J. Climate, revised.*
- Murakami, H., R. Mizuta, and E. Shindo, 2011: Future changes in tropical cyclone activity projected by multi-physics and multi-SST ensemble experiments using 60-km mesh MRI-AGCM. *Clim. Dyn.* In press.
- Murakami, H., B. Wang, and A. Kitoh, 2011: Future change of western North Pacific typhoons: Projections by a 20-km-mesh global atmospheric model. *J. Climate*, **24**, 1154–1169.
- Murakami, H., and B. Wang, 2010: Future change of North Atlantic tropical cyclone tracks: Projection by a 20-km-mesh global atmospheric model. *J. Climate*, **23**, 2699–2721.
- Murakami, H. and M. Sugi, 2010: Effect of model resolution on tropical cyclone climate projections. *SOLA*, **6**, 73–76.

Future changes in TC frequency and genesis frequency



Dynamic factors have high correlations, indicating these dynamic parameters are of primary importance for the future changes in TC genesis global distribution.

MPI (Maximum Potential Index)



$$MPI^2 = \frac{C_k T_s}{C_D T_0} \left(CAPE^* - CAPE^b \right)$$

where C_k is the exchange coefficient for enthalpy, C_D is the drag coefficient, T_s is the SST (K), and T_0 is the mean outflow temperature (K). The quantity $CAPE^*$ is the value of convective available potential energy (CAPE) of air lifted from saturation at sea level, with reference to the environmental sounding, and $CAPE_b$ is that of the boundary layer air.

Both quantities are evaluated near the radius of maximum wind which is theoretically determined.

In recent years, TCs become more active.

·Hurricane activity in the North Atlantic (NA)

showed an increase over the past 30 years.

Hurricane Katrina (2005) : the most damaging storm in USA

Hurricane Rita (2005) : the most intense (895 hPa) TC

observed in the Gulf of Mexico

Hurricane Wilma (2005) : the most intense (882 hPa) TC in NA

·Abnormal TC number in the western North Pacific in 2004.

·Typhoon Morakot in 2009 caused catastrophic damage in Kaohsiung in Taiwan.

Previous studies have proposed that these recent changes are due to global warming.

Emanuel, 2005; Anthes et al., 2006; Hoyos et al., 2006; Mann and Emanuel, 2006; Trenberth and Shea, 2006; Holland and Webster, 2007; Mann et al., 2007a; Mann *et al.*, 2007b

However, this view has been challenged by the following points:

a) The observation before satellite era (before 1979) is not reliable.

Landsea *et al.*, 2006; Landsea, 2007

b) Recent increases in the frequency of NA TCs are within the range of multi-decadal variability.

Pielke *et al.*, 2006; Bell and Chelliah, 2006

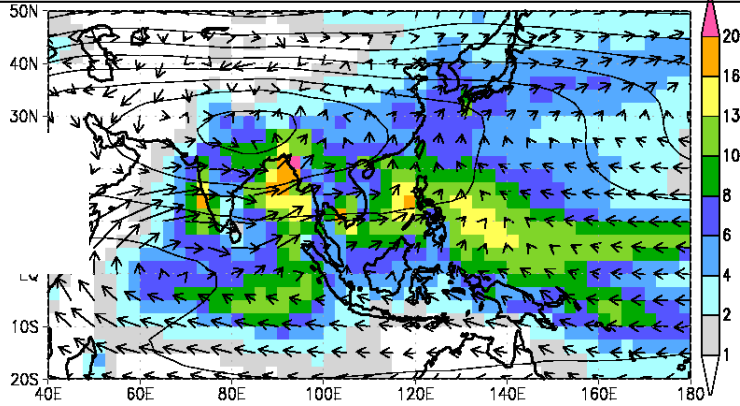
c) Projections by climate models are not reliable because the models are too coarse to resolve TC structures.

Goldenberg et al. 2001.

TC scale is 100–1000 km, while typical horizontal resolution of climate models is 100–300 km mesh.

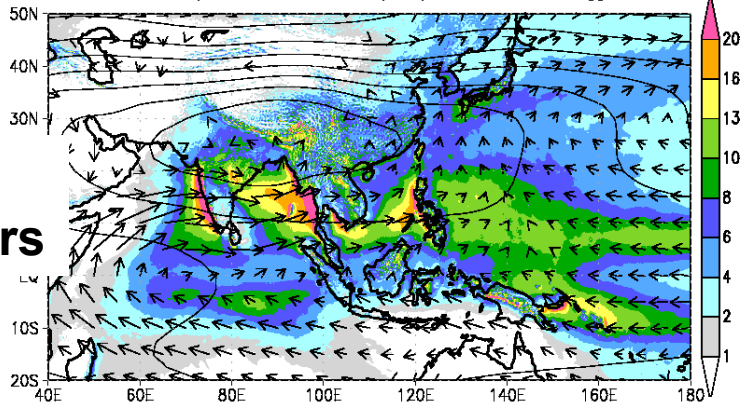
Asian summer monsoon (JJA mean)

JRA25+CMAP (z200-z500)+pr+uv850 jja



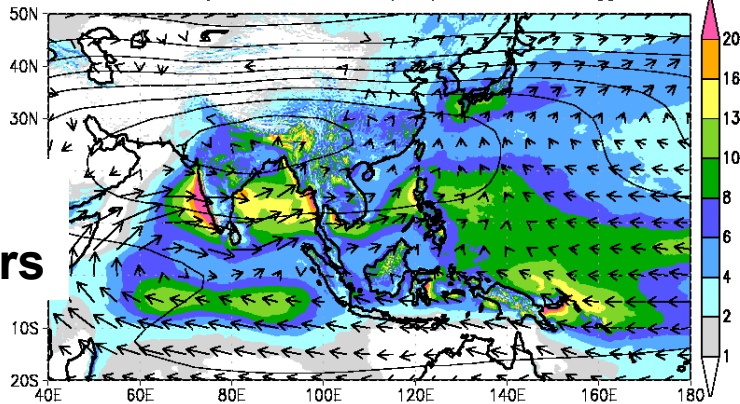
OBS (JRA + CMAP)

SPA (z200-z500)+pr+uv850 jja



**New Model
20km25years**

SP0A (z200-z500)+pr+uv850 jja

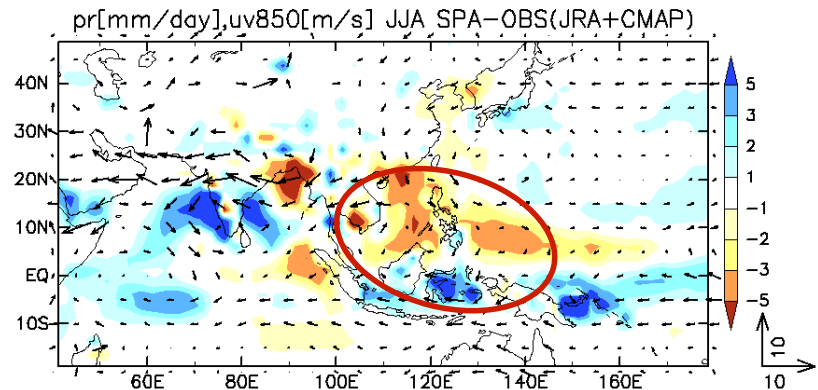
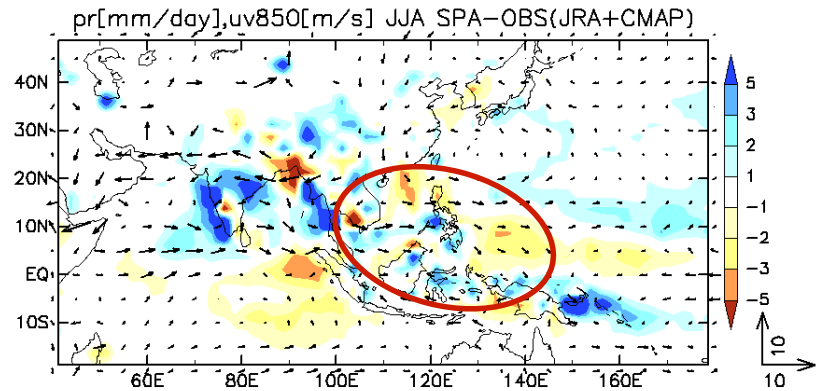


**Prev Model
20km25years**

→ cint=50m

**Colors: Precipitation
Arrows: 850hPa wind
Contours: Thickness(200-500hPa)**

diff from OBS



Skill score of 25-year climatology

- Skill Score by Taylor (2001)

σ : standard deviation
(model/obs),
R: correlation coefficient

Global			Jan		Jul	
variable	vs	region	v3.1	v3.2	v3.1	v3.2
Precip	CMAP	Global	0.7716	0.803	0.7862	0.8189
Precip	GPCP	Global	0.746	0.7814	0.7429	0.7566
Z500	JRA25	Global	0.9928	0.997	0.9951	0.9943
SLP	JRA25	Global	0.9322	0.9735	0.9529	0.9533
T850	JRA25	Global	0.9949	0.995	0.9908	0.9943
U850	JRA25	Global	0.9363	0.9651	0.9435	0.9401
U200	JRA25	Global	0.958	0.9702	0.9648	0.9778
V200	JRA25	Global	0.8198	0.8584	0.7758	0.8085
Netrad	ERBE	Global	0.9577	0.9714	0.9499	0.9644
OLR	ERBE	Global	0.9387	0.9503	0.9425	0.9539
OSR	ERBE	Global	0.8778	0.9076	0.855	0.8873
GZ5eddy	JRA25	Global	0.8918	0.9145	0.8108	0.8503
SLPeddy	JRA25	Global	0.9062	0.9137	0.871	0.8909
T850eddy	JRA25	Global	0.9401	0.9443	0.9291	0.9342
U850eddy	JRA25	Global	0.8433	0.8629	0.8722	0.9028
U200eddy	JRA25	Global	0.8959	0.9154	0.8463	0.9137

Asia			Jan		Jul	
variable	vs	region	v3.1	v3.2	v3.1	v3.2
Precip	TRMM3B4	Asia	0.7724	0.8153	0.3886	0.497
Precip	CMAP	Asia	0.7378	0.8034	0.4523	0.5616
Precip	GPCP	Asia	0.6488	0.7468	0.3441	0.4088
Z500	JRA25	Asia	0.9823	0.9806	0.7266	0.7813
SLP	JRA25	Asia	0.9553	0.9562	0.7894	0.8836
T850	JRA25	Asia	0.9676	0.9632	0.9195	0.9776
U850	JRA25	Asia	0.9387	0.9454	0.8395	0.8547
U200	JRA25	Asia	0.9849	0.9944	0.8866	0.9641
V200	JRA25	Asia	0.5805	0.4717	0.7945	0.7923
GZ5eddy	JRA25	Asia	0.8594	0.9162	0.8161	0.868
SLPeddy	JRA25	Asia	0.8744	0.8817	0.8185	0.902
T850eddy	JRA25	Asia	0.8837	0.8654	0.8785	0.936
U850eddy	JRA25	Asia	0.8633	0.8683	0.8393	0.8833
U200eddy	JRA25	Asia	0.9216	0.95	0.7995	0.9217

- Better at **New Model**
- Better at **Prev Model**

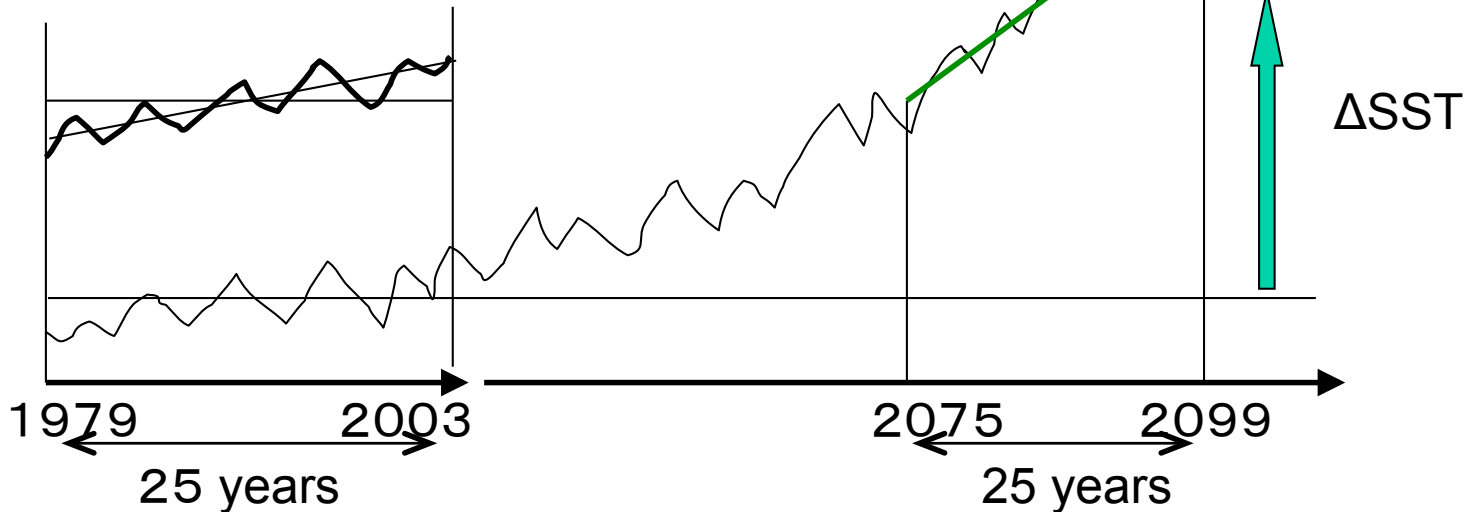
How to prescribe SST

Mizuta et.al (2008)

Present SST

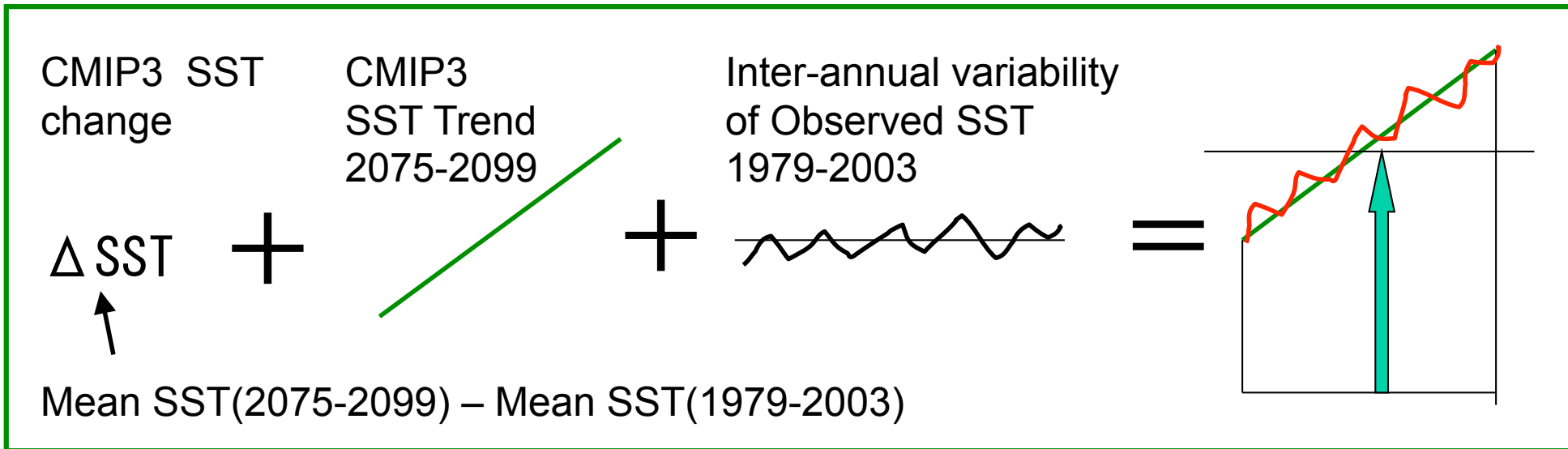
Observed SST
1979~2003

AR4_20thCentury
Exp. SST -2001



Future SST

also applies for 2015-2039



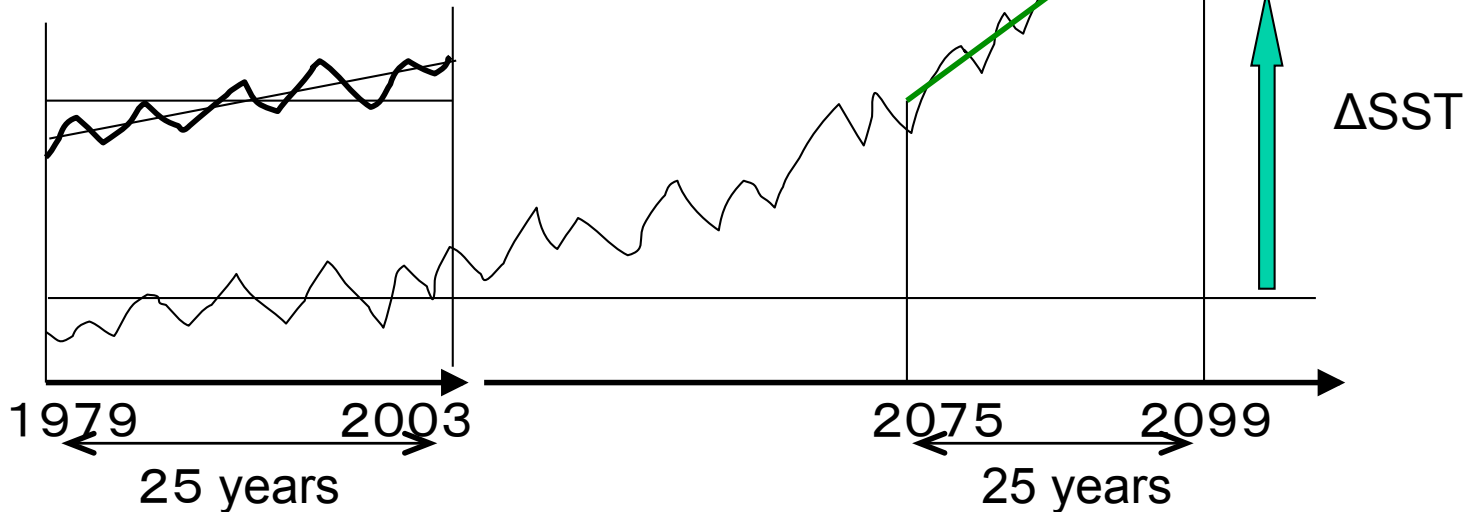
How to prescribe SST

Mizuta et.al (2008)

Present SST

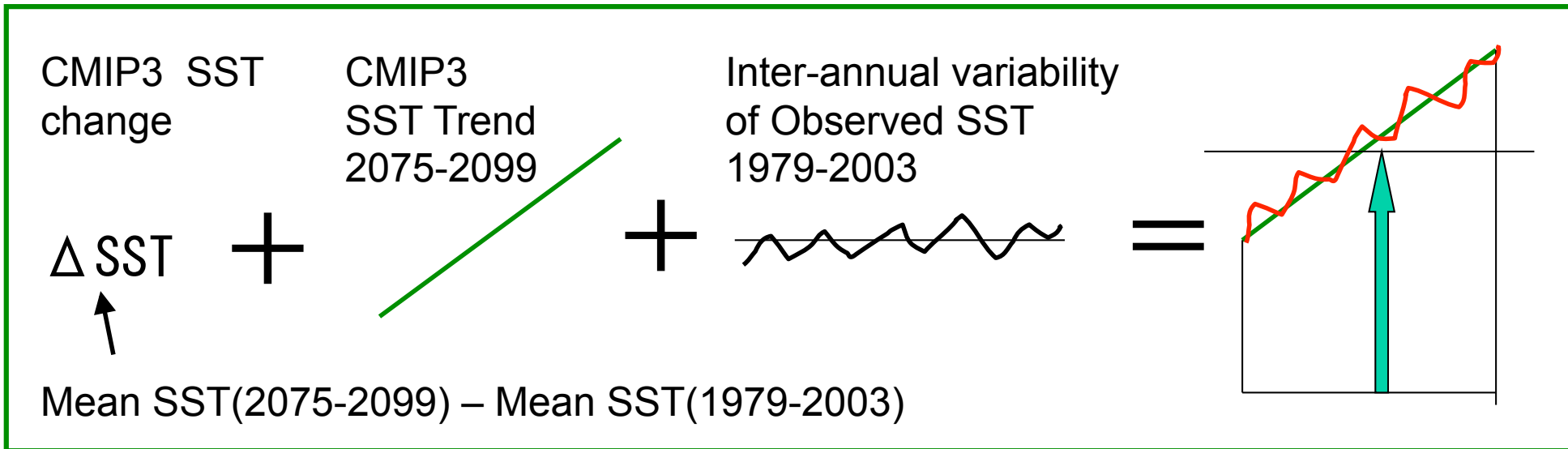
Observed SST
1979~2003

AR4_20thCentury
Exp. SST -2001



Future SST

also applies for 2015-2039





Multi-SST Ensemble Projections using 60-km-mesh model

- 1) For each CMIP3 model, a mean future change in SST is computed by subtracting the 1979-2003 mean SST from the 2075-2099 mean SST.
- 2) The computed mean future change in SST is normalised by dividing by the tropical mean (30°S-30°N) future change in SST.
- 3) The normalised value for each model is subtracted from the multi-model ensemble mean of the normalised value.
- 4) The inter-model pattern correlation r of the normalised values is computed between each pair of models.
- 5) Norms (or distances) are defined as $2 \times (1 - r)$ for each model, and the cluster analysis is performed using these norms.
- 6) When the final three groups are bounded, the clustering procedure is terminated.

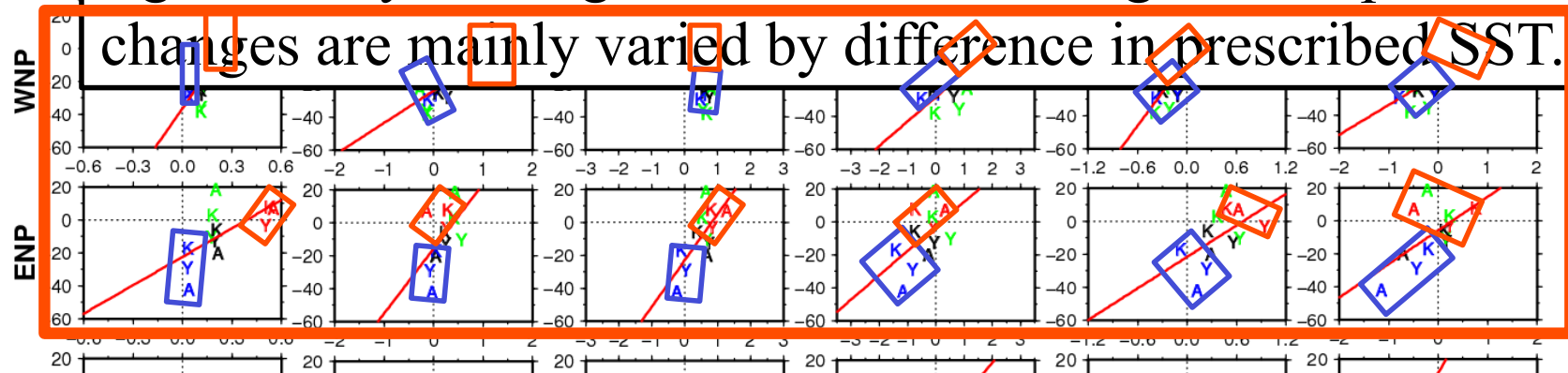


Factors responsible for Inter-experiment differences

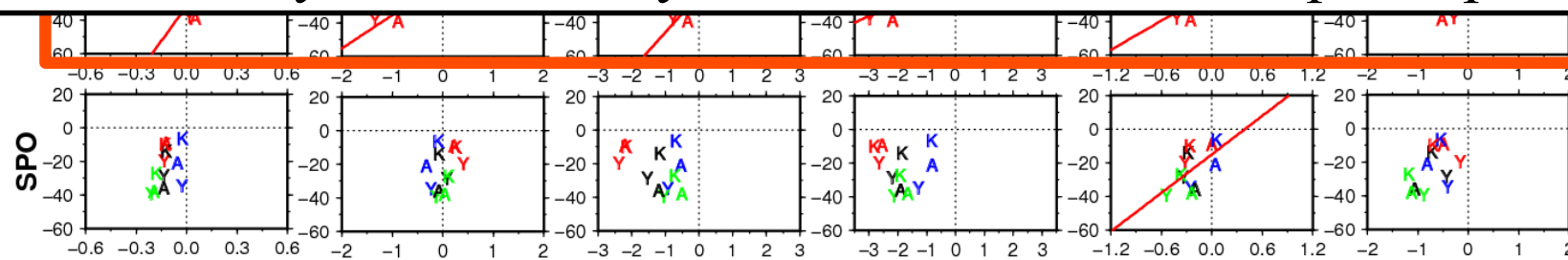
Y: YS, K: KF, A: AS, black: CMIP3 mean, blue:C1, green:C2, red:C3

δS_a [K] $\delta \eta_{850}$ [$10^{-6} s^{-1}$] $-\delta V_s$ [m s $^{-1}$] $-\delta V_{zs}$ [m s $^{-1}$] $-\delta \omega_{500}$ [$10^{-2} Pa s^{-1}$] δD [$10^{-10} s^{-2}$]

GL
NIO
Difference in dynamical parameters are highly correlated with TGF difference among the experiments in the WNP, ENP, and SIO, indicating the difference in future changes in dynamical parameters are primary source of uncertainty.



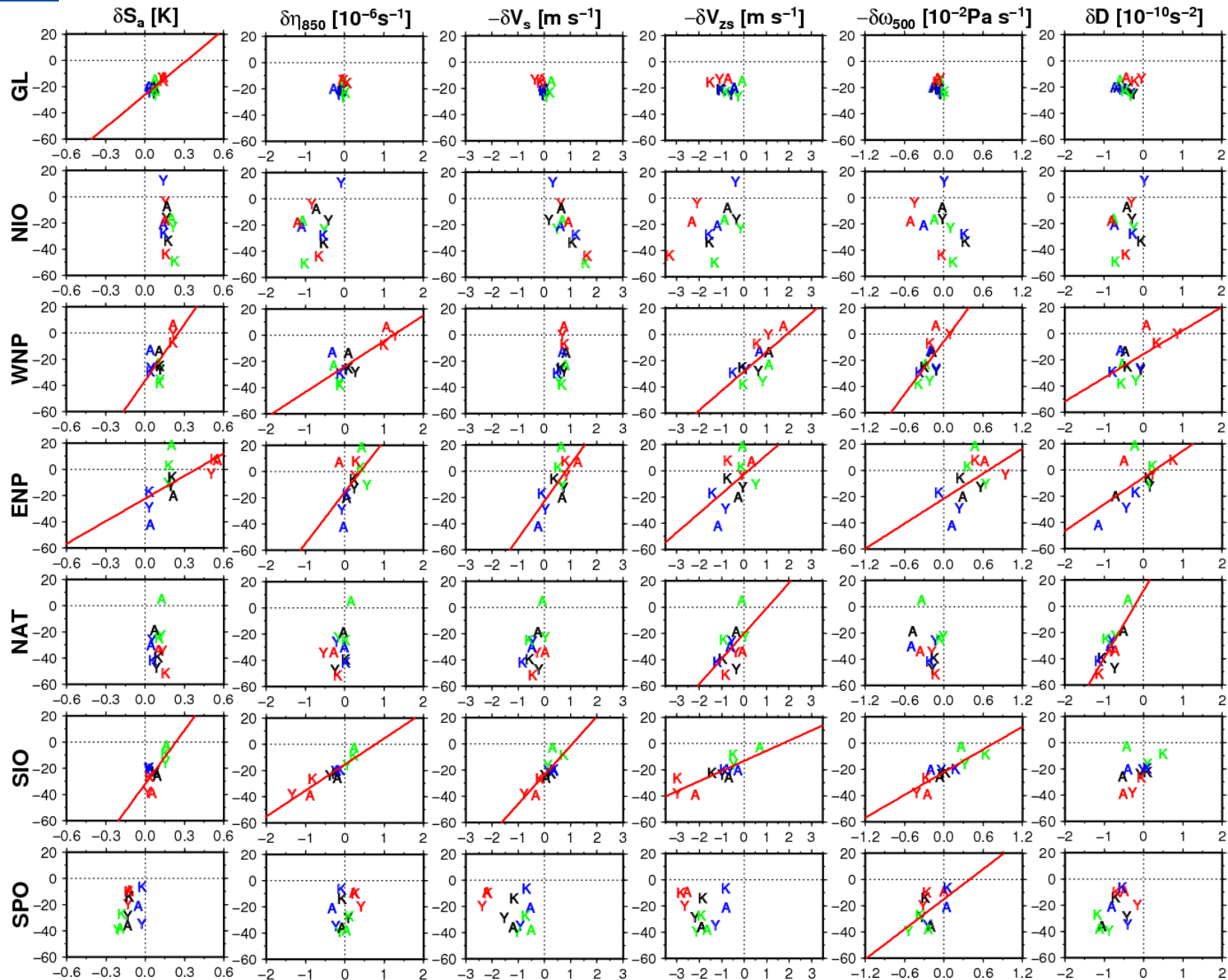
The experiments with identical prescribed SSTs are eccentrically located in the panels, indicating that the dynamical parameters are more heavily influenced by differences in the SST spatial patterns.



Factors responsible for Inter-experiment differences

Y: YS, K: KF, A: AS,

black: CMIP3 mean, blue:C1, green:C2, red:C3



Factors responsible for Inter-experiment differences

	δS_a	δRH	δV_{pot}	$-\delta\chi$	$-\delta\Gamma_d$	$\delta\eta_{850}$	$-\delta V_s$	$-\delta V_{zs}$	$-\delta\omega_{500}$	δD
		Thermodynamic				Dynamic				
GL	0.70	-0.22	0.15	0.13	-0.66	0.22	-0.31	-0.28	-0.36	0.08
NH	0.75	0.24	0.74	0.41	-0.70	0.53	0.69	0.44	0.15	0.40
SH	0.47	-0.27	-0.06	-0.21	-0.04	0.60	0.64	0.43	0.69	-0.03
NIO	-0.48	0.33	0.31	0.40	-0.14	0.33	-0.81	0.44	-0.39	0.34
WNP	0.66	0.06	-0.06	0.23	-0.78	0.78	0.49	0.68	0.63	0.61
ENP	0.64	-0.00	0.58	-0.11	-0.43	0.51	0.72	0.51	0.51	0.62
NAT	-0.00	0.48	0.22	0.59	-0.65	0.43	0.41	0.50	-0.29	0.78
SIO	0.71	0.40	0.50	0.28	-0.47	0.91	0.83	0.83	0.83	0.40
SPO	0.45	-0.78	-0.21	-0.52	-0.31	0.35	-0.42	-0.10	0.57	0.43

Dynamic factors have high correlations, indicating these dynamic parameters are of primary importance for the inter-experimental differences.